Dielectric and Conduction Mechanisms of Parylene N at High Temperature: Phase-Transition Effect

ARTICLE *in* THE JOURNAL OF PHYSICAL CHEMISTRY A · MAY 2015

Impact Factor: 2.69 · DOI: 10.1021/acs.jpca.5b01379 · Source: PubMed

4 AUTHORS, INCLUDING:

Achraf Kachroudi
TIMA Laboratory
3 PUBLICATIONS **2** CITATIONS
SEE PROFILE

Abdel Kahouli
National Graduate School of Engineering and …
36 PUBLICATIONS **122** CITATIONS
SEE PROFILE

THE JOURNAL OF PHYSICAL CHEMISTRY A

Article

pubs.acs.org/JPCA

Dielectric and Conduction Mechanisms of Parylene N at High Temperature: Phase-Transition Effect

Achraf Kachroudi,*[,†] Abdelkader Kahouli,[†] Julien Legrand,[‡] and Fathi Jomni[†]

[†]Laboratoire Matériaux Organisation et Propriétés (LMOP), Université de Tunis El Manar, 2092 Tunis, Tunisia

[‡]RADIALL Centr'alp Z.I. Centr'alp-642, Rue E. Romanet, BP 35-38341 Voreppe, France

ABSTRACT: Dielectric and electrical properties correlated with the structure analysis have been studied on 27% semicrystalline parylene-N ($-H_2C-C_6H_4-CH_2-)_n$ thin films. Transition-phase, AC- and DC-conduction mechanisms, and the MW-interfacial polarization were identified in parylene N at high temperature by experimental and theoretical investigations. The dielectric analysis based on the dc conductivity highlights a temperature of 230 °C as a transition temperature from the α-form to the β_1-form. This structure transition is accompanied by a modification on the DC-conduction mechanisms from ionic to electronic conduction in the α-form and the β_1-form, respectively. The AC conduction mechanism is governed by the small polaron tunneling mechanism (SPTM) with $W_{H,\alpha}$ = 0.23 eV and a tunneling distance of 7.71 Å in the α-form, while it becomes a correlated barrier-hopping (CBH) mechanism with a W_{M,β_1} = 0.52 eV in the β_1-form. The imaginary part of the electrical modulus formalism obeys the Kohlrausch–Williams–Watt (KWW) model and shows the presence of the interfacial polarization effect. The theoretical Kohlrausch exponent (β_{KWW}) confirms the existence of the transition phase on the parylene N in the vicinity of the 230 °C as deduced by the DC- and the AC-conduction parameters. The correlations between the experimental results and the theoretical models are very useful knowledge and tools for diverse parylene N applications at high temperature.

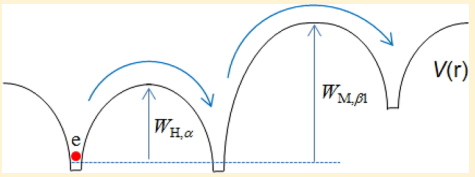

INTRODUCTION

Poly-*p*-xylylene, parylene N (also named Pa-n), constitutes the basic element of the parylene family series. This polymer appears as a very good candidate for many applications in the industrial domain. The success found with this material is essentially thanks to its excellent physical, chemical, biological[1] and electrical properties.[2,3]

Developent of elaboration techniques for this semicrystalline polymer and the conditions optimization of the manufacturing process named CVD (chemical vapor deposition)[1,4] give this material a good surface conformity and uniformity in a large area of substrates. For this reason, parylene N appears to be a very good barrier for humidity[5] and several other environments.[6] These properties make parylene N very attractive as an insulating material in recent applications; it serves as a coating layer of the inner surfaces of microfluidic channels made from PDMS (poly dimethylsiloxane) to inhibit the fluorescent substance absorption circulating in channels.[7]

In addition, parylene N can be used in the field of sensors,[8] for example, as an electrochemical passivation coating layer realized for silicon-nanowire-based sensors in intracellular biochemical detection.[8] This coating layer aims to minimize electrical losses and electrical noise and avoid redox reactions in the metal's surfaces in the sensors.

Recently, parylene N was also used as a micromembrane in capacitive sensor arrays for chemical and biological applications.[9]

A common reason why this material is chosen for these last applications is the maintenance of its electric and dielectric properties (low and fixed dielectric constant and also good insulation) after the manufacturing process. Nevertheless, the dielectric properties of the polymer can be affected by the frequency variation of the electric field and by variation of the temperature.

It is known that parylene N shows a polymorphism crystalline structure,[6,10−12] and it is interesting to study the electrical properties in each crystalline form from T_g[13] to the β_2-form. The aim of this work is to study and understand the dielectric properties in large temperature and frequency ranges. The ac-conductivity behavior on the same range of temperature is also fulfilled. A correlation between the theoretical and experimental results gives more information to understand the electrical conduction mechanisms in the material.

We use the model of electric modulus to accentuate the interfacial polarization in this semicrystalline polymer.[14] These investigations will indicate the reliability of using this material in the microelectronics field over a large temperature and frequency range.

EXPERIMENTAL SECTION

Sample Preparation. Parylene N is obtained from a cyclic dimer (di-*p*-xylylene) by the commercial Gorham process,[15] also called CVD. This material is deposited on Inox 316L substrate at room temperature. The deposition process is made in three main stages: The first stage consists of sublimation to transform the solid dimer directly in the gas phase at a

Received: February 10, 2015
Revised: May 18, 2015

DOI: 10.1021/acs.jpca.5b01379
J. Phys. Chem. A XXXX, XXX, XXX−XXX

temperature of 130−160 °C and a pressure of 0.5 mbar. Then, the obtained gaseous molecules pass in a furnace pyrolysis chamber at a temperature of 650−700 °C and a pressure of 0.1 mbar. The dimer gaseous molecules are totally converted to monomers (Figure 1). The last stage is the polymerization:

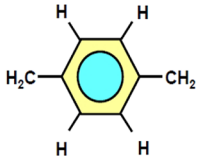

Figure 1. Chemical structure of the parylene N monomer.

monomers coming from pyrolysis settle via polymerization on the substrate at ambient temperature and a pressure of 0.02 mbar. The advantage of this process is the ability to obtain thin films with good homogeneity and conformability.[1] The obtained films for this study are 5.6 μm thickness. For the dielectric characterizations, the Inox 316L (substrate) will serve as a bottom electrode. In order to constitute the metal−insulator−netal for dielectric characterizations, a thin gold film is deposited on parylene N as a top electrode.

X-ray Diffraction. XRD measurement was realized on parylene N thin films by using a high-resolution (θ–θ) BRUKER D8 ADVANCE diffractometer equipped with an X-ray tube with copper anticathode Cu Kα (λ = 1.540562 Å, 40 kV, 30 mA). The diffraction diagram is obtained from 5° to 30° in 2θ with a 0.02° step and a 2 s counting time. The collected data allowed us to calculate the crystallographic parameters of the parylene N structure and especially the degree of crystallinity of this polymer.

Dielectric Measures. The equipment used to study the electrical and dielectric properties is composed of the following experimental devices: a surrounding wall working under primary vacuum sector and under inert gas (nitrogen) to avoid the sample contamination by oxygenated elements during the measurement, and a temperature regulator (LINKAM TM S94) and an impedance analyzer (SOLARTRON 1260) are coupled with a dielectric interface on 1296 for the measures. Parylene N in an MIM configuration was polarized with an alternating voltage of 100 mV. The frequency study is from 10^{-1} to 10^{5} Hz, and the sample temperature measurement changes from 190 to 270 °C in steps of 20 °C. The stabilization time was equal to 10 min at each temperature.

THEORETICAL BACKGROUND

Generally, the dielectric system response submitted to an external alternative electric field is governed, in the frequency domain, by the complex permittivity formalism (eq 1).

$$\varepsilon^*(\omega, T) = \varepsilon'(\omega, T) - i\varepsilon''(\omega, T) \tag{1}$$

$\varepsilon'(\omega, T)$ and $\varepsilon''(\omega, T)$ are the real and imaginary parts of the complex permittivity, which represent the storage and the losses of the energy respectively during every electric field cycle. This formalism of complex permittivity was widely used by several authors to identify the relaxation phenomenon in oxides and polymers. It also constitutes a way to prove the various contributions to the conductivity in materials. However, in the case of the semicrystalline polymers, the relaxation processes analysis through this formalism is difficult, especially at low frequencies and high temperatures because the dc-conductivity phenomenon hides any relaxation process.[14] To overcome this problem, we introduce the electric modulus formalism that is defined as the inverse of the relative complex permittivity $\varepsilon^*(\omega, T)$.

$$M^*(\omega, T) = \frac{1}{\varepsilon^*(\omega, T)} = M'(\omega, T) + iM''(\omega, T) \tag{2}$$

$M'(\omega, T)$ and $M''(\omega, T)$ represent, respectively, the real and imaginary parts of the electric modulus, which can be defined from eq 1.

$$M'(\omega, T) = \frac{\varepsilon''(\omega, T)}{\varepsilon''^2(\omega, T) + \varepsilon''^2(\omega, T)} \tag{3}$$

$$M''(\omega, T) = \frac{\varepsilon''(\omega, T)}{\varepsilon''^2(\omega, T) + \varepsilon''^2(\omega, T)} \tag{4}$$

The nonexponential conductivity relaxation could be expressed using the Kohlrausch−Williams−Watt (KWW) model.[16]

$$M^*_{\beta_{KWW}}(\omega, T) = M_\infty\left[1 - \int_0^\infty e^{i\omega t}\frac{-\mathrm{d}\phi}{\mathrm{d}t}\mathrm{d}t\right] \tag{5}$$

with

$$\phi(t) = \phi_0 e^{(-t/\tau_\sigma)^{\beta_{KWW}}} \tag{6}$$

which represents the electric field wihin the material. M_∞ represents the $M'(\omega, T)$ asymptotic value, and τ is the conductivity relaxation time. β_{KWW} is the Kohlrausch exponent with the condition $0 \leq \beta_{KWW} \leqslant 1$.

Bergman[17,18] gave a modified KWW function for fitting approach in the frequency domain and the imaginary part of the electric modulus, which can be expressed by eq 7

$$M''(\omega) = \frac{M''_{max}}{(1-\beta_{KWW}) + \left(\frac{\beta_{KWW}}{1+\beta_{KWW}}\right)\left(\beta_{KWW}\frac{f_{max}}{f} + \left(\frac{f}{f_{max}}\right)^{\beta_{KWW}}\right)} \tag{7}$$

where M''_{max} is the maximum peak of the imaginary part of the electric modulus and f_{max} is the corresponding peak frequency. Furthermore, for a given temperature and the study frequency domain, the ac conductivity could be calculated according to the relation[19−21]

$$\sigma^*(\omega, T) = i\varepsilon_0\omega\varepsilon^*(\omega, T) = \varepsilon_0\omega\varepsilon''(\omega, T) + i\varepsilon_0\omega\varepsilon'(\omega, T) \tag{8}$$

The real part of $\sigma^*(\omega, T)$ is given by

$$\sigma_{ac}(\omega, T) = \varepsilon_0\omega\varepsilon''(\omega, T) \tag{9}$$

where $\varepsilon_0 = 8.85 \times 10^{-12}$ F·m^{-1} is the free space permittivity, and $\omega = 2\pi f$ the angular frequency. The σ_{ac} can be expressed also as eq 10

$$\sigma_{ac}(\omega, T) \sim \omega^{n(T)} \tag{10}$$

This relation represents the electric conductivity described by the Jonscher power law model, and $n(T)$ represents the power exponent which depends on the temperature satisfying the condition $0 \leq n(T) \leq 1$.

DOI: 10.1021/acs.jpca.5b01379
J. Phys. Chem. A XXXX, XXX, XXX−XXX

RESULTS AND DISCUSSION

The semicrystalline nature of the parylene N samples exploited during our measures is confirmed by X-ray powder diffraction (Figure 2). From the XRD pattern, we determined the

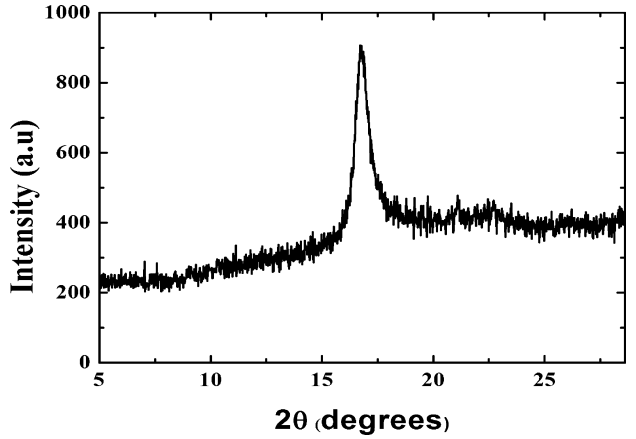

Figure 2. XRD pattern of the parylene N at ambient temperature (α-form).

elementary cell parameters of the parylene N structure and a 27% of crystallinity of this polymer. At room temperature, parylene N crystallizes in monoclinic form (the parameters are summarized in Table 1). This structure represents the α-form

Table 1. Lattice Parameters and the Main Structure Properties of Parylene N (α-Form)

sample	a (Å)	b (Å)	c (Å)	β	grain size (nm)	crystallinity (%)
Pa-n	9.6498	5.2266	6.3369	132.8°	23.56	27

of parylene N, which was revealed by other authors.[6,12] This information from the XRD proves that parylene N is in its semicrystalline state in the temperature study domain as are the other parylene families.[2,22]

The dielectric constant ε' and the dielectric loss ε'' vary as a frequency function from 10^{-1} to 10^{5} Hz as shown in Figures 3 and 4 at the temperature range from 190 to 270 °C.

ε'' shows a particular behavior; in fact, ε'' increases considerably at high temperature and at low frequencies

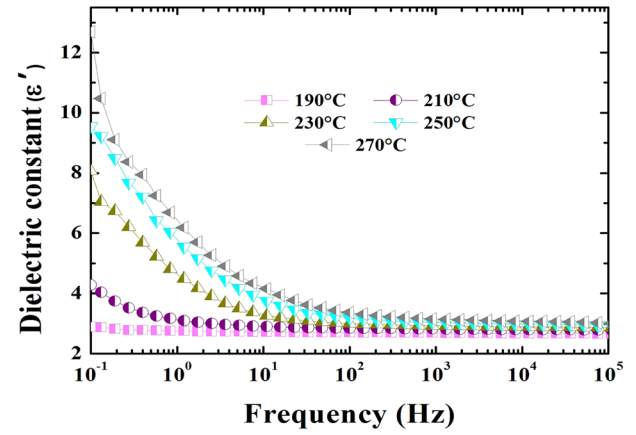

Figure 3. Dielectric constant against frequency at various temperatures ranging from 190 °C to 270 °C.

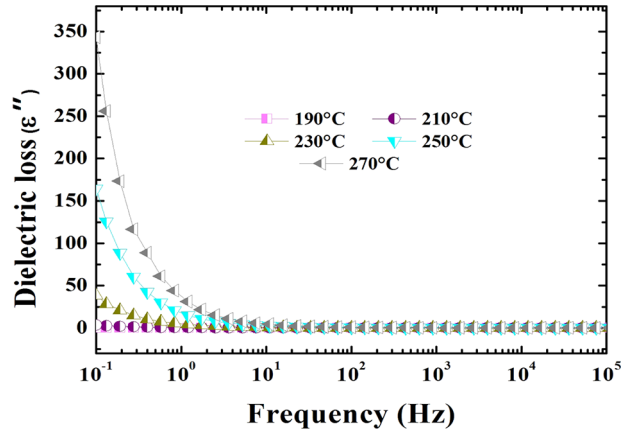

Figure 4. Dielectric losses against frequency at various temperatures ranging from 190 to 270 °C.

between 10^{-1} and 10 Hz. The slope of ε'' according to the frequency is equal to −1 at low frequencies. By considering the dielectric physics theory, these dielectric losses are related to the DC-conduction contribution in the material σ_{dc}. This contribution can be expressed in the losses through eq 11.

$$\varepsilon''_{dc} = \frac{\sigma_{dc}}{\varepsilon_0 \omega} \tag{11}$$

This equation can explain the origin of the slope −1.

We can represent the conductivity of the σ_{ac} in the material using eq 9. The σ_{ac} as a function of the frequency and the temperature is represented in Figure 5.

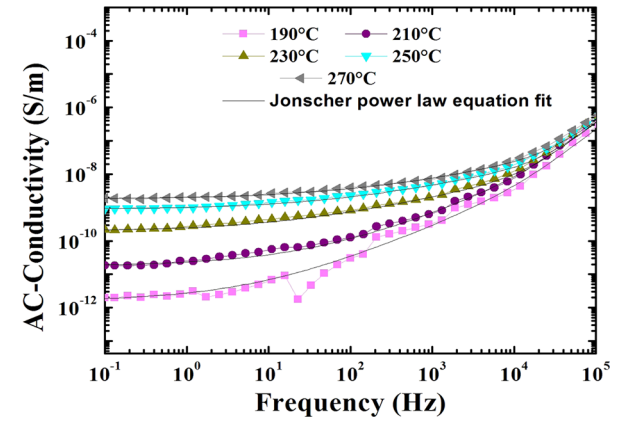

Figure 5. Frequency dependence of the conductivity of parylene N.

The parylene N conductivity can be described by the "Jonscher power law", which is expressed by eq 12

$$\sigma_{ac} = \sigma_{dc} + A\omega^{n(T)} + B\omega \tag{12}$$

where σ_{dc} is the low-frequency conductivity, A and B are pre-exponent constants which depend essentially to the temperature, and $n(T)$ is the exponent power law which is also temperature-dependent.

At low frequencies, the conductivity is independent of the frequency; these values in the plateau appearing in the considered region are characteristic of the DC-conduction σ_{dc} that inscreases with the temperature. The DC conduction can be explained by the phenomenon of jumping carrier conduction at long ranges.[2] In addition, at high frequencies,

DOI: 10.1021/acs.jpca.5b01379
J. Phys. Chem. A XXXX, XXX, XXX−XXX

σ_{ac} shows a dependent-frequency behavior that can be described by the two other terms of eq 12. This part shows a very low influence in temperature. This phenomenon is attributed to the jumping carrier conduction but at short range,[2] which can be controlled by the external electric field applied to the material.

By using eq 12, $n(T)$ and σ_{dc} are computed for various temperatures ranging from 190 to 270 °C as represented in Figures 6 and 7.

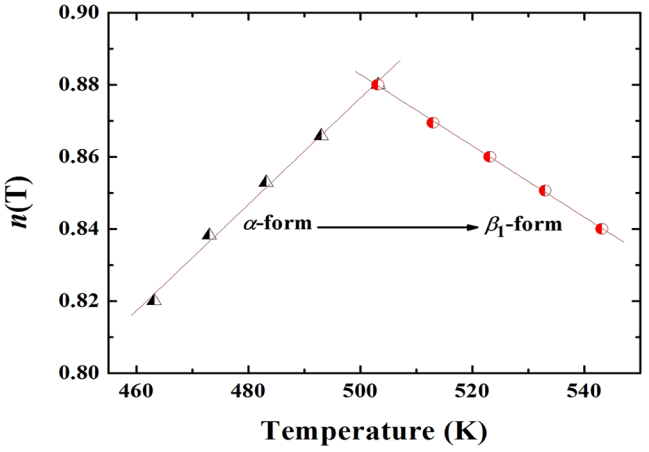

Figure 6. Exponent power law $n(T)$ versus temperature ranging from 190 to 270 °C (from 463.15 to 543.15 K) .

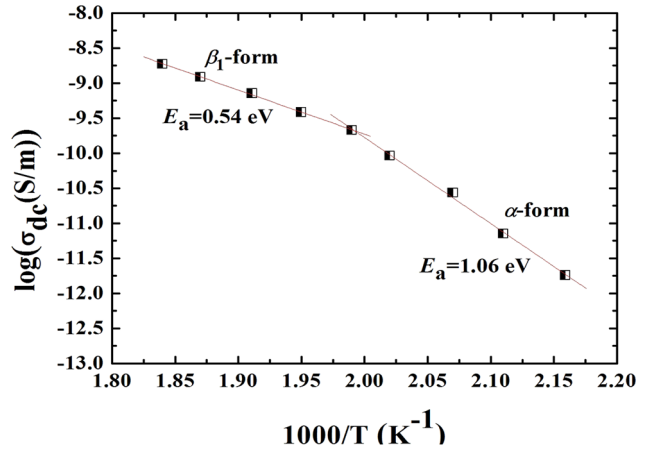

Figure 7. Arrhenius plot of σ_{dc} as a function of temperature.

Figure 6 shows the temperature dependence of the exponent $n(T)$. We find a very particular behavior, in fact; the curve has a maximum at around 230 °C (≃ 503 K) separating two regions with different behavior. According to the many previous works with different structural techniques, this temperature corresponds to the $\alpha-\beta_1$ phase transition in parylene N.[6,10−12] Figure 7 shows that the conductivity σ_{dc} obeys the Arrhenius law, which is given by eq 13

$$\sigma_{dc} = \sigma_0 \exp\left(-\frac{E_a}{k_b T}\right) \tag{13}$$

where σ_0 is a constant, T is the absolute temperature, k_b is the Boltzmann constant, and E_a is the process activation energy. σ_{dc} shows a discontinuity in the values observed at a temperature around 230 °C (≃ 503 K) accompanied by two linear regions with different activation energies which are plotted in Figure 7; this behavior is in good agreement with the results obtained from the Jonscher law exponent ($n(T)$).

To more understand the parylene N response at high temperature, the material is annealed at the obtained transition temperature (230 °C ≃ 503 K) for 12 h. Figure 8 shows the XRD pattern of the annealed sample.

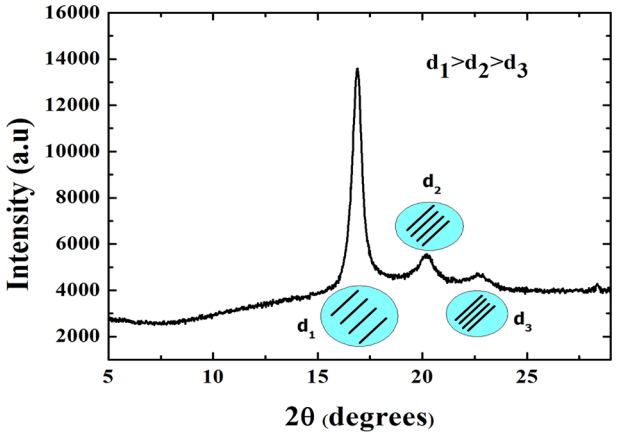

Figure 8. XRD pattern of the parylene N annealed at 230 °C (≃ 503 K) (β_1-form).

The XRD pattern analysis (Figure 8) shows that parylene N has undergone a crystallographic change from the α (monoclinic) to the β_1 (hexagonal) phase at 230 °C, and this has been demonstrated by other authors.[10,11] This change at this temperature greatly affects the electrical and dielectric properties of the polymer (Figures 6 and 7). The β_1 phase lattice parameters are summarized in Table 2.

Table 2. Lattice Parameters and the Main Structure Properties of Parylene N (β_1-Form)

sample	a (Å)	c (Å)
Pa-n	20.47	6.55

It clearly seems that after the postannealing of the material, two supplementary peaks at 2θ = 20.21° and 2θ = 22.70° appear at the higher diffraction angle with a slow increase of the (200) peak (2θ = 16.89°) of the as deposited parylene N.

According to the Bragg equation (eq 14), the presence of three different peaks on the XRD pattern of the annealed parylene N means that this material exhibited three different package chains as shown by the schematic schemes (Figure 8). The intramolecular distance of the package chain decreases by increasing the diffraction angle, showing that the annealing process ensures the molecular arrangement

$$2d \sin\theta = q\lambda \tag{14}$$

where q is the diffraction order, d is the interchains distance, λ is the wavelength, and θ is the diffraction angle.

In addition, the annealing process induces more crystalline with small sizes than that obtained from the as-deposited sample basing on the Debye Sherrer formula (eq 15)

$$\delta = \frac{K\lambda}{\mathrm{FWHM}\cos\theta} \tag{15}$$

DOI: 10.1021/acs.jpca.5b01379
J. Phys. Chem. A XXXX, XXX, XXX−XXX

where K = constant = 0.9, θ is the diffraction angle, and δ is the grain size.

We can deduce that the annealing process favors the germination phenomenon more than growth because the 2θ diffraction angle of the as-deposited parylene N does not change after the annealing process, while it permits the appearance of two others peaks. According to our knowledge of the structure studies carried out on parylene N, crystallographic orientations of the two additional diffraction peaks appear after the annealing processes of parylene N are not known in the literature. More refine structural studies are needed to identify precisely and clearly their unit cells and their lattice planes. This work is the subject of a future structure study of the β_1-form in our researcher groups. Indeed, in the present work we considered these peaks as a qualitative structure element to understand the electrical results of parylene N at high temperature.

Now, we go back on the curve $n(T)$. For low temperatures, we note that n increases with temperature reaching a maximum value; this suggests that the interaction between the charges involved in the conduction phenomenon in the polymer and between the charges and the lattice in the α phase is important and increases with temperature. Once the temperature of 230 °C is reached, parylene N is transformed to the β_1-form, and this last structure induces a considerable increase of the electrical conductivity as shown by the decreasing barrier height of the potential wells. In that condition, the conduction mechanisms on parylene N at low frequency can be correlated to an ionic conduction mechanism via deep traps (1.06 eV) in the α-form, and it becomes an electronic conduction mechanism occurring in shallow traps (0.54 eV). On the basis of the X-ray diffraction pattern results (Figure 8) in relation to the obtained electrical conduction mechanisms (Figure 7), the additional diffraction peaks obtained in the β_1-form after the annealing process can be treated in an electrical image as an additional of a conductive compound with more packed electrical charges in the material since the electrical conductivity is abruptly increased and the barrier height of the DC conductivity (low frequency regime) is decreased. In the higher frequencies regime (AC conductivity) of the measured electrical conductivity where the conduction response of parylene N can be described by the Jonscher law equation (eq 12), it is interesting to quantify the exponent value ($n(T)$) in order to understand the main conduction mechanisms occurring in the material. As shown in Figure 6, the value of $n(T)$ increases as a function of temperature until 503 K in the α-form.

From the theories existing in the literature[22] to explain AC conductivity in disordered materials, it appears that the above trend of data for $n(T)$ is indicative of a small polaron tunneling mechanism (SPTM). Considering this approach, the small polaron[22] can be seen as being formed with the amorphous/crystal interfaces or they can be formed mainly in the amorphous phase of the materials (disordered portion) which constitutes the most significant phase (73%). According to this model, we have the formula expressed by eq 16 and 17.

$$n = 1 - \frac{4}{\left[\ln\left(\frac{1}{\omega\tau_0}\right) - \frac{W_{H,\alpha}}{k_b T}\right]} \tag{16}$$

$$R_\omega = \frac{1}{2\alpha}\left[\ln\left(\frac{1}{\omega\tau_0}\right) - \frac{W_{H,\alpha}}{k_b T}\right] \tag{17}$$

In the above equations, α^{-1} is the spatial extension of the polaron, R_ω is the tunelling distance, τ_0 is the characteristic relaxation time, $W_{H,\alpha}$ is the polaron hopping energy. The experimental values of $n(T)$ at various temperatures were fitted to eq 16, taking $W_{H,\alpha}$ as the parameter. The value of τ_0 is considered to be 10^{-13} s.[22] The values of $W_{H,\alpha}$ can be calculated from eq 16 by using the slope of the line in graph $(1 - n(T))$ versus T for the α-form and were found to be equal to 0.23 eV. For τ_0 of 10^{-13} s, f = 1 kHz, α = 1 Å^{-1}[22] and $W_{H,\alpha}$ = 0.23eV, the value of the AC parameter R_ω at the temperature T = 190 °C = 463.15 K is of 7.71 Å. The tunneling distance R_ω in the SPTM is in the order of few units of the interatomic spacing.

According to the correlated barrier hopping (CBH) model, the values of the frequency exponent $n(T)$ extend from 0.7 to 1 and prove to decrease with the increase in the temperature.[22] This model is in good agreement with our experimental results for the β_1-form, thus suggesting that the electrical AC conduction mechanism of parylene N at high temperature can be explained by charge-carrier hops between sites over the potential barrier W_{M,β_1} separating them. From this model, the frequency exponent $n(T)$ is evaluated by eq 18[22]

$$n = 1 - \frac{6k_b T}{W_{M,\beta 1}} \tag{18}$$

where $W_{M,\beta 1}$ is the height of maximum barrier (or binding energy) which must surmount the charges trapped in localized sites (deep trap), τ_0 is the characteristic relaxation time which is in the order of an atom vibrational period ($\tau_0 \sim 10^{-12}$ s),[22] and $W_{M,\beta 1}$ is calculated in experiments starting from the linear line slope which is between $(1 - n(T))$ and T (Figure 9). A value of

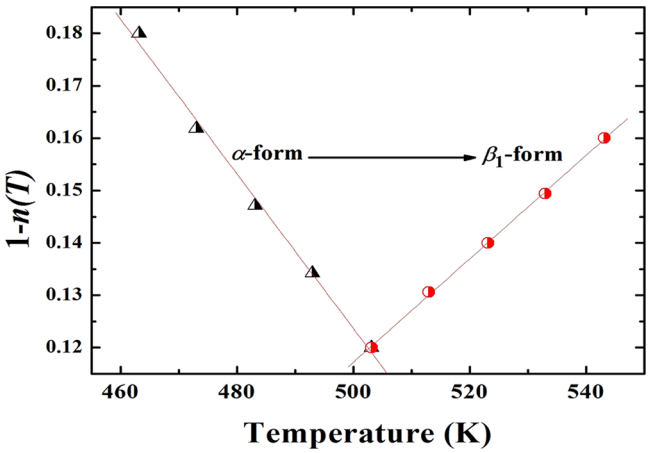

Figure 9. Variation of the parameter $(1 - n(T))$ with temperature.

$W_{M,\beta 1}$ = 0.52 eV is obtained for parylene N. For this model, the $W_{M,\beta 1}$ is practically 2 orders of magnitude higher than the calculated $W_{H,\alpha}$ for the α-form as shown by the schematic model illustration in Figure 10.

As our work is focused on the higher temperature regime, some relaxations phenomena can be masked by the ionic conduction effect at low frequencies basing on the complex relative permittivity formalism. The dispersion phenomenon and the high dielectric losses (Figure 4) observed at low-frequency and high-temperature regions on the real and the

DOI: 10.1021/acs.jpca.5b01379
J. Phys. Chem. A XXXX, XXX, XXX−XXX

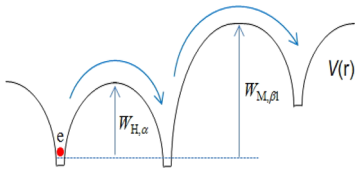

Figure 10. Schematic model of the AC-conduction mechanism in the α-form and β_1-form in parylene N.

imaginary parts of the relative permittivity (Figure 3), respectively, are a sign of mixture effects of polarization and conduction mechanisms.

In order to dissociate both electrical behaviors responsible of the high value of the real and the imaginary (Figure 4) part of the relative permittivity at low frequency, the electrical modulus formalism is used.

Two phenomena can explain the origin of the dielectric constant growth: interfacial polarization (Maxwell−Wagner−-Sillars) and ion conductivity. XRD study confirms that throughout the temperature range study the parylene N is in its semicrystalline form with a crystallinity of 27%. This structure supports the presence of a polarization at the amorphous/crystalline regions surfaces (interfacial polarization). The problem is that this polarization in polymer is usually masked by the conductivity effect on ε'' (Figure 4). To overcome this problem and to study the two phenomena separately, we propose to use the electric modulus formalism which is widely used in this type of study.[2,23]

The complex electric modulus M^*, its real and imaginary part, are calculated from eqs 2−4, respectively. From a physical point of view, the electrical modulus corresponds to the electric field relaxation in the polymer when the electric displacement field is constant and represents the real dielectric relaxation process. The dielectric data recorded are subsequently transformed into M' and M'' via the equations mentioned above.

We can observe from Figure 11 that M' tends to zero at low frequencies for the study temperatures; this phenomenon can be attributed to the ionic conductions. For high frequencies, M' reaches a limit value $M_\infty' = 1/\varepsilon_\infty$, which is characteristic of a relaxation phenomenon.

The M'' curves in Figure 12 for different temperatures show clearly peaks for characteristic relaxation frequencies. Relaxation

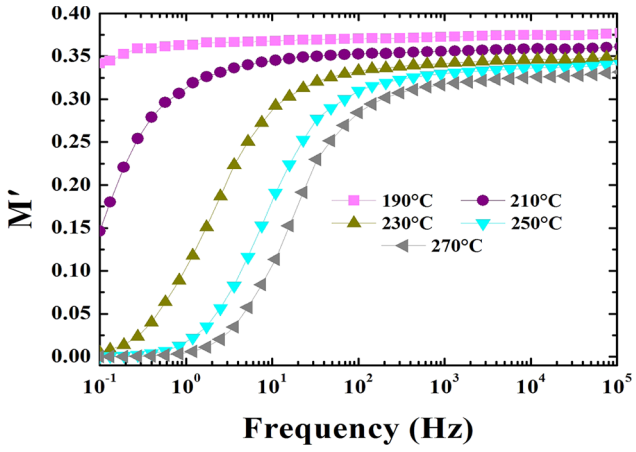

Figure 11. Real part M' of the electric modulus for temperatures ranging from 190 °C to 270 °C.

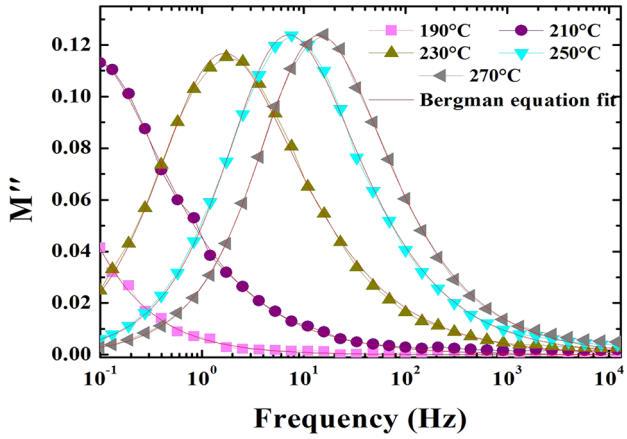

Figure 12. Bergman equation fit of M'' for temperatures ranging from 190 to 270 °C.

peaks are shifted toward higher frequencies by increasing the temperature; this suggests that this phenomenon is associated with thermally activated process. The frequency regime below the peak position M'' indicates a movement of carriers over long distances showing an existence of MWS polarization. At the frequencies above that of the peak, carriers are spatially confined to potential wells and free to move within the wells and the dipoles do not have time to be reoriented according to the electric field and the interfacial polarization do not show an effect on the dielectric response. The frequency range where the peak occurs is suggestive of the transition from long to short-range mobility.

We propose fitting the curves in Figure 12 by eq 7. The fitting allows us to identify M''_{max}, f_{max}, and β_{KWW} on each curve for temperatures ranging from 190 to 270 °C. Table 3 summarizes the values of the constants resulting from fitting.

Table 3. Parameter Values Resulting from the Bergman Equation Fit

temp (K)	M_{max}''	f_{max}	β_{KWW}
463	0.12374	0.01177	0.84645
483	0.11582	0.07897	0.67087
503	0.11678	1.66627	0.6662
523	0.12395	7.14944	0.70565
543	0.12375	14.20282	0.72235

From the values in Table 3, we represent the variations of the coefficient β_{KWW} against the temperature and the Arrhenius plot showing the variations of f_{max} against the temperature too are given in Figures 13 and 14, respectively.

From Figure 13, we find that the stretched exponential parameter β_{KWW} has a minimum at about 492.52 K. In fact, we have already seen that there is a phase transition at 503 K and thus the variation of β_{KWW} may be affected by this transition existing in parylene N. This allows us to conclude that the relaxation process dynamics are different from both sides of the phase-transition temperature. Moreover, considering the variations of structures starting from a monoclinic cell to an hexagonal lattice,[3] we can confirm that the interfacial relaxation is reinforced in the second variant supposing that the charge carriers become more popular after the annealing process.

From Figure 14, we find that the interfacial polarization obeys the Arrhenius law expressed by eq 19

DOI: 10.1021/acs.jpca.5b01379
J. Phys. Chem. A XXXX, XXX, XXX−XXX

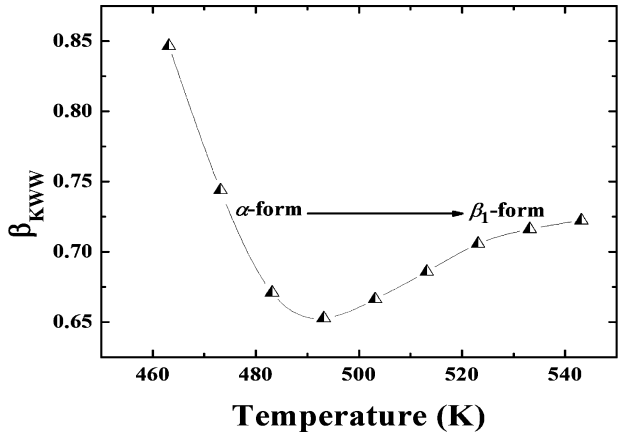

Figure 13. Variation of stretched exponential parameter β_{KWW} with temperature.

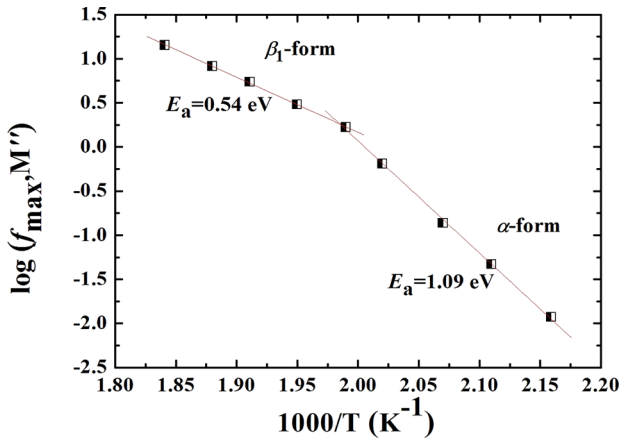

Figure 14. Arrhenius plot of f_{max} as a function of temperature.

$$f_{max} = f_0 \exp\left(-\frac{E_a}{k_b T}\right) \quad (19)$$

where f_0 is a constant.

This polarization represents a discontinuity at the transition temperature already studied with different activation energies on either side of this temperature which are given in Figure 14. The Maxwell−Wagner−Sillars relaxation results of the residual charge carriers mobility in the material condensing at amorphous/crystalline interfaces. The lowest activation energy of the β_1-form confirms that the interfacial polarization is promoted and achieved more easily in the hexagonal configuration since this structure exhibits three different cystalline package chains as shown by the XRD pattern (Figure 8). In addition, these activation energies values are in good agreement with those already calculated for the DC conductivity, which confirms that these two phenomena are activated simultaneously and therefore governed by the same charges carrier.

CONCLUSION

Structure, dielectric, and electrical properties of semicrystalline parylene N films were studied at high temperature from 190 to 270 °C in a large frequency range varying from 0.1 Hz to 100 kHz. XRD and dielectric spectroscopy analyses are correlated to several theoretical models in order to investigate the main relaxation and AC/DC conduction mechanisms in the material. A transition phase is detected by the dielectric analysis in the vicinity of 230 °C, which is correlated to the transformation of the material from the α-form (monoclinic) to the β_1-form (hexagonal). This structural transition is obtained by a post annealing of the material at 230 °C for 12 h. The AC-conduction mechanisms (high-frequency regime) of parylene N are governed by a small polaron tunneling mechanism (SPTM) with $W_{H,\alpha}$ = 0.23 eV in the α-form and by a correlated barrier hopping (CBH) mechanism with a W_{M,β_1} = 0.52 eV in the β_1-form. At low-frequency regimes corresponding to DC conduction, the conductivity exhibits a discontinuity behavior at 230 °C, consistent to the transition phase. It shows a transition of the DC-conduction mechanism from a deep trap (1.06 eV) in the α-form to a shallow trap (0.54 eV) in the β_1-form. The structure−properties relationships based on the association of the experimental results with the theoretical models elucidate with precisely the main transition phase and the AC/DC-conduction mechanisms in parylene N films.

AUTHOR INFORMATION

Corresponding Author

*E-mail: achraf.kachroudi.ens@gmail.com.

Notes

The authors declare no competing financial interest.

REFERENCES

(1) Jeffrey, F. B., Toh-Ming, L. *Chemical Vapor Deposition Polymerization: The Growth and Properties of Parylene Thin Films*; Kluwer Academic Publishers: Dordrecht, 2003.

(2) Kahouli, A.; Sylvestre, A.; Jomni, F.; Yangui, B.; Legrand, J. Ac-Conductivity and Dielectric Relaxations Above Glass Transition Temperature for Parylene-C Thin Films. *Appl. Phys. A: Mater. Sci. Process.* **2012**, *106*, 909−913.

(3) Kahouli, A.; Sylvestre, A.; Pairis, S.; Laithier, J. F. Effect of Cl-H Aromatic Substitution on Structural and Dielectric Properties of Poly(p-xylylene). *Polymer* **2012**, *53*, 3001−3007.

(4) Zhang, X.; Dabral, S.; Chiang, C.; Mcdonald, J. F.; Wang, B. Crystallinity Properties of Parylene-n Affecting Its Use as An ILD in Submicron Integrated Circuit Technology. *Thin Solid Films* **1995**, *270*, 508−511.

(5) Christopher, D. W. J., Glen, D. W. *Non-Hermetic Packaging for Lithium Niobate-Based Devices*; Agere Systems, Inc.: Allentown, 2003.

(6) Lee, S. *Kirk−Othmer Encyclopedia of Chemical Technology*; John Wiley and Sons: New York, 1983.

(7) Sasaki, H.; Onoe, H.; Osaki, T.; Kawano, R.; Takeuchi, S. Parylene-Coating in PDMS Microfluidic Channels Prevents The Absorption of Fluorescent Dyes. *Sens. Actuators, B* **2010**, *150*, 478−482.

(8) Park, I.; Li, Z.; Li, X.; Pisano, A. P.; Williams, R. S. Towards the Silicon Nanowire-Based Sensor for Intracellular Biochemical Detection. *Biosens. Bioelectron.* **2007**, *22*, 2065−2070.

(9) Satyanarayana, S.; McCormick, D. T.; Majumdar, A. Parylene Micro Membrane Capacitive Sensor Array for Chemical and Biological Sensing. *Sens. Actuators, B* **2006**, *115*, 494−502.

(10) Niegisch, W. D. Crystallography of Poly-p-xylylene. *J. Appl. Phys.* **1966**, *37*, 4041−4046.

(11) Isoda, S.; Tsuji, M.; Ohara, M.; Kawguchi, A.; Katayamara, K. Structural Analysis of β-Form (P-xylylene) Starting from a High-Resolution Image. *Polymer* **1983**, *24*, 1155−1161.

(12) Iwamoto, R.; Wunderlich, B. Crystal Structure of Poly-p-xylylene. I. The α Form. *J. Polym. Sci., Polym. Phys.* **1973**, *11*, 2403−2411.

(13) Streltsov, D. R.; Grigor'ev, E. I.; Dmitryakov, P. V.; Erina, N. A.; Mailyan, K. A.; Pebalk, A. V.; Chvalun, S. N. Initial Stages of Growth of Poly(p-xylylene) Coatings: AFM Study. *Polym. Sci., Ser. A* **2009**, *51*, 881−890.

DOI: 10.1021/acs.jpca.5b01379
J. Phys. Chem. A XXXX, XXX, XXX−XXX

(14) Kremer, F., Schönhals, A., Luck, W. *Broadband Dielectric Spectroscopy*; Springer-Verlag: New York, 2002.
(15) Gorham, W. F. A new, General Synthetic Method for the Preparation of Linear Poly-p-xylylenes. *J. Polym. Sci., Part A-1: Polym. Chem.* **1966**, *4*, 3027−3039.
(16) El Hasnaoui, M.; Graça, M. P. F.; Achour, M. E.; Costa, L. C. Electric Modulus Analysis of Carbon Black/Copolymer Composite Materials. *Mater. Sci. Appl.* **2011**, *2*, 1421−1426.
(17) Bergman, R. General Susceptibility Functions for Relaxations in Disordered Systems. *J. Appl. Phys.* **2000**, *88*, 1356.
(18) Moynihan, C. T.; Boesch, L. P.; Laberge, N. L. Decay Function for the Electric Field Relaxation in Vitreous Ionic Conductors. *Phys. Chem. Glasses* **1973**, *14*, 122−125.
(19) Jonscher, A. K. *Universal Relaxation Law*; Dielectrics Press: London, 1992.
(20) Jonscher, A. K. Relaxation in Low-Loss Dielectrics. *J. Mol. Liq.* **2000**, *86*, 259−268.
(21) Jonscher, A. K. *Dielectric Relaxation in Solids*; Dielectrics Press: London, 1983.
(22) Kahouli, A.; Sylvestre, A.; Jomni, F.; Yangui, B.; Legrand, J. Experimental and Theoretical Study of AC Electrical Conduction Mechanisms of Semicrystalline Parylene C Thin Films. *J. Phys. Chem. A* **2012**, *116*, 1051−1058.
(23) Kahouli, A.; Sylvestre, A.; Lutsen, L.; Laithier, J. F.; Pairis, S.; André, E.; Garden, J. L. Structural and Dielectric Properties of Parylene-VT4 Thin Films. *Mater. Chem. Phys.* **2014**, *143*, 908−914.

DOI: 10.1021/acs.jpca.5b01379
J. Phys. Chem. A XXXX, XXX, XXX−XXX